

Published in final edited form as:

Nanomedicine. 2011 October ; 7(5): 595–603. doi:10.1016/j.nano.2011.01.013.

Fe₃O₄ nanoparticles with daunorubicin induce apoptosis through Caspase-8/PARP pathway and inhibit K562 leukemia cell-induced tumor growth *in vivo*

Gen Zhang, MS^{1,3}, Bin Bin Lai, MD², Yan Yan Zhou, BS¹, Bao An Chen, MD², Xue Mei Wang, PhD^{1,*}, Qun Lu, PhD³, and Yan-Hua Chen, PhD^{3,*}

¹ State Key Lab of Bioelectronics (Chien-Shiung Wu Lab), Department of Biological Science and Medical Engineering Southeast University, Nanjing, 210096, P. R. China

² Zhongda Hospital and School of Clinic Medicine, Southeast University, Nanjing, 210009, P.R. China

³ Department of Anatomy and Cell Biology, East Carolina University Brody School of Medicine, Greenville, NC 27834, USA

Abstract

Nanomaterials can enhance the delivery and treatment efficiency of anti-cancer drugs, but the mechanisms of the tumor-reducing activity of Fe₃O₄ nanoparticles with daunorubicin have not been established. Here we investigate the synergistic effects of Fe₃O₄ nanoparticles with daunorubicin on the induction of apoptosis using K562 leukemia cells. Fe₃O₄ nanoparticles increased the ability of daunorubicin to induce apoptosis in both adriamycin-sensitive and adriamycin-resistant K562 cells through Caspase-8/Poly (ADP-ribose) polymerase pathway. Fe₃O₄ nanoparticles combined with daunorubicin also effectively inhibited the tumor growth induced by the inoculation of K562 cells into nude mice. The increased cell apoptotic rate was closely correlated with the enhanced inhibition of tumor growth. Biodistribution studies in xenograft tumors indicated that Fe₃O₄ nanoparticles could be potentially excreted from the body via the gastrointestinal system. In conclusion, our study suggests that Fe₃O₄ nanoparticles combined with anti-cancer drugs could serve as a better alternative for the targeted therapeutic approaches to cancer treatments.

Keywords

Nanoparticles; Apoptosis; Leukemia K562 cells; Biodistribution; Caspase-8

© 2011 Elsevier Inc. All rights reserved.

*Correspondence: Xue Mei Wang, State Key Lab of Bioelectronics (Chien-Shiung Wu Lab), Department of Biological Science and Medical Engineering, Southeast University, Nanjing, 210096 P. R. China, Tel: 025-83792177, xuewang@seu.edu.cn. Yan-Hua Chen, Department of Anatomy and Cell Biology, East Carolina University Brody School of Medicine, Greenville, NC 27834, USA, Tel: 252-744-1341 Fax: 252-744-2850, chen@ecu.edu.

Publisher's Disclaimer: This is a PDF file of an unedited manuscript that has been accepted for publication. As a service to our customers we are providing this early version of the manuscript. The manuscript will undergo copyediting, typesetting, and review of the resulting proof before it is published in its final citable form. Please note that during the production process errors may be discovered which could affect the content, and all legal disclaimers that apply to the journal pertain.

Background

The treatment efficiency of cancer chemotherapy depends not only on the anti-cancer drug itself but also on how it is delivered to the targets.¹ Polymer nanospheres and nanoparticles have been increasingly investigated as drug delivery systems to enhance the drug delivery efficiency to cancer cells.^{2–5} The combination of anti-tumor drugs with nanomaterials can potentially overcome the non-cellular and cellular-based mechanisms of drug resistance and increase the selectivity of drugs toward cancer cells while reducing their toxicity toward normal tissues.

Daunorubicin (DNR) is one of the most effective anti-cancer drugs on the market today.⁶ However, one of the biggest shortcomings of DNR is its low anti-tumor activity against adriamycin-resistant K562 (KA) cells.⁷ In order to increase the therapeutic efficiency and reduce the side-effects, DNR in the presence of tetraheptylammonium-coated Fe₃O₄ nanoparticles has been used to improve its anti-tumor activity.² Anti-cancer drugs combined with magnetic nanoparticles can be injected into the bloodstream and guided to specific body sites with external magnetic fields.⁸ This method, if well-established, could reduce the systemic toxicity of chemotherapeutic agents and require a much lower dose of anti-cancer drugs to achieve the treatment efficiency. Until today, the mechanism of tumor-reducing activity of DNR with Fe₃O₄ has not been validated in adriamycin-resistant K562 (KA) cells. Additional confirmation of DNR with Fe₃O₄ delivery into cancer cells and their excretion out of the body is also lacking.

Due to the unique properties of Fe₃O₄ nanoparticles, such as good biocompatibility, super-paramagnetic property, low toxicity, and relatively easy preparation,^{9–10} we further investigated the biological effects of Fe₃O₄ nanoparticles alone as well as combined with DNR in this study. In drug-sensitive K562 and drug-resistant KA cells, we found that Fe₃O₄ nanoparticles greatly increased the DNR sensitivity against cancer cells and induced apoptosis through Caspase-8/Poly (ADP-ribose) polymerase (PARP) pathway. The *in vivo* study also revealed that Fe₃O₄ nanoparticles with DNR showed remarkable efficacies to inhibit KA cell-induced tumor growth in nude mice when the magnet was fixed securely onto the tumor region to create external magnetic fields. We have further examined the tissue distributions of Fe₃O₄ nanoparticles in nude mice. Atomic absorption spectroscopy revealed that Fe content was markedly higher in the liver, intestine, and tumor compared to that of the control groups. These studies suggest that metal Fe in the hepatocyte secretory pathway could be excreted mostly via the gastrointestinal system.

Materials and Methods

(See additional information on online Methods and Experimental Details)

Preparation of Fe₃O₄ Nanoparticles

Fe₃O₄ nanoparticles were prepared using the EDOC method as described previously.¹ Briefly, the electrolysis processes were carried out in 0.1 mol/L tetraheptylammonium dissolved in the 2-propanol solution using the anode of high-purity Fe sheets and cathode of glassy carbon. A current density of 10–40 mA/cm² was applied for electrolysis. The deposited clusters were capped with tetraheptylammonium, which acted as a stabilizer of the colloidal nanocrystallites. Following deposition, a hydrothermal treatment was taken to improve the composition and structure.

IC₅₀ analysis by MTT cell viability assay

The 50% of K562 and KA cell growth inhibitory concentration of DNR, Fe₃O₄, and Fe₃O₄ plus DNR were calculated as IC₅₀ values (see Supplemental Materials for MTT assay). In

addition, Fe₃O₄ nanoparticles and DNR combination index (CI) was determined using the classic isobologram equation of Chou and Talalay: $CI = (a/A) + (b/B)$, where a is the DNR IC₅₀ in combination with Fe₃O₄ at the concentration b ; A is the IC₅₀ of DNR without Fe₃O₄ and B is the IC₅₀ of Fe₃O₄ in the absence of DNR. According to this equation, when $CI < 1$, the interaction is synergistic; when $CI = 1$, the interaction is additive; when $CI > 1$, the interaction is antagonistic.¹¹

Acridine Orange/Ethidium Bromide (AO/EB) staining to detect apoptosis

K562 and KA cells were seeded in 6-well plates (5×10^5 /well) and incubated in the presence of 1.99×10^{-6} mol/L of DNR, 0.58 mg/L of Fe₃O₄ nanoparticles, or the same Fe₃O₄ concentration with 1.99×10^{-6} mol/L of DNR for 72 hours. To stain apoptotic cells, the plates were centrifuged for 5 min before adding AO/EB dye mixture (100 µg/ml acridine orange and 100 µg/ml ethidium bromide) to each well. Cells were viewed under the fluorescent light microscope.

Experimental animals

Animal studies were approved by the institutional animal care and use review committee of Southeast University. The female nude mice (6-week old) were purchased from the Animal Feeding Farm of National Institute for the Control of Pharmaceutical and Biological Products (P. R. China). All mice were housed in the animal facility, and animal experiments (See Online Experimental Details) that were conducted followed the guidelines by the Animal Research Ethics Board of Southeast University. Animals were kept in the facility with free access to food and water.

In situ apoptosis by TUNEL staining

Apoptotic cell death in deparaffinized tumor tissue sections was detected using terminal deoxynucleotidyl transferase-mediated dUTP nick end-labeling (TUNEL) with the Klenow DNA fragmentation detection kit (Roche, USA). Apoptotic cells were identified by the dark brown nuclei observed under a light microscope. Three slides were generated from each tumor in each group, and then ten fields from each slide were randomly selected to make the statistical analysis.

Statistical analysis

Results were presented as Mean \pm SD. A t-test was performed in each group for each time point. A value of $P < 0.05$ was considered statistically significant.

Results

Fe₃O₄ nanoparticles increase the DNR-elicited growth inhibition of K562 and KA cells

First, we used transmission electron microscopy (TEM) to characterize the Fe₃O₄ nanoparticles. Figure 1A shows the TEM images of the Fe₃O₄ nanoparticles. The average size of nanoparticle is about 30 nm. The nanoparticles were also characterized with Dynamic Light Scattering (DLS), which measured the hydrodynamic diameter of the nanoparticles in their dispersion state. The mean size of Fe₃O₄ nanoparticles measured in the culture medium was about 80 ± 5.3 nm (Fig. 1B). We also measured iron (III) in the culture medium containing the working concentration of Fe₃O₄ nanoparticles. We found that within the time course in which our routine experiments were conducted, the amount of iron (III) in the culture medium was very small and could be neglected (see Online Supplemental Materials).

The MTT assay was carried out to examine the cell growth inhibition after K562 and KA cells were treated with various concentrations of DNR, Fe₃O₄ nanoparticles, or Fe₃O₄ nanoparticles with different concentrations of DNR for 36 hours (Fig. 1C and D, Supplemental Material S1). As shown in Fig. 1C, K562 cell viability was significantly reduced with the increasing concentrations of DNR, Fe₃O₄ nanoparticles, or Fe₃O₄ nanoparticles combined with DNR. Therefore, all treatments elicited cytotoxicity on K562 cells in a dose-dependent manner. The cell growth inhibition rate was higher when treated with 0.58 mg/L Fe₃O₄ nanoparticles and different concentrations of DNR than those treated with just DNR (Fig. 1C).

Since KA is a drug-resistant cell line, increasing DNR concentrations for KA cells did not increase the growth inhibition rate at the same magnitude as it did for K562 cells (Fig. 1D). Significantly, in comparison to DNR alone treatment, the growth inhibition rate was increased when KA cells were treated with 0.58 mg/L Fe₃O₄ nanoparticles and with different concentrations of DNR. The IC₅₀ values of each treatment were calculated as shown in Table 1. The IC₅₀ value of DNR for KA cells [(39.72±2.95)×10⁻⁶ mol/L] was about five-fold higher compared to that of K562 cells [(7.94±0.76)×10⁻⁶ mol/L]. This is due to the fact that KA cells are a multidrug resistant cell line and less sensitive to the DNR treatment. It requires a much higher concentration of drug to achieve 50% inhibitory effect. Next, we carried out the combination study and results are presented in Table 2. The results revealed that Fe₃O₄ nanoparticles and DNR combination index (CI) of K562 and KA cells were 0.67 and 0.26, respectively. This clearly showed the significant enhancement of the cell inhibition rate by the synergistic effect of Fe₃O₄ nanoparticles with DNR to leukemia cells, especially to the drug-resistant leukemia KA cells.

The growth of K562 and KA cells after treated with Fe₃O₄, DNR, or Fe₃O₄ plus DNR was also examined (Supplemental Material S2). The results were consistent with the cell growth inhibition assay (Fig. 1C and D) in that the number of cells was reduced in a dose-dependent manner in each treatment on both cell lines. In addition, Fe₃O₄ plus DNR treatment was more effective than treatment with Fe₃O₄ or DNR alone (S2, A and B). The most striking observation was that the KA cells were more sensitive to DNR after they were treated with DNR combined with Fe₃O₄, and the resistant fold was significantly declined. The reversal ability of Fe₃O₄ nanoparticles on KA was illustrated in Table 3. Without Fe₃O₄ nanoparticles, the resistant factor was 5.00 for KA, while addition of 0.58 mg/L Fe₃O₄ nanoparticles significantly decreased the resistant factor by 84% to 0.8. The reversal index of KA cells to Fe₃O₄ nanoparticles was 6.25 (Table 3). These analyses demonstrate that Fe₃O₄ nanoparticles plus DNR treatments were more effective on suppressing KA cell growth than Fe₃O₄ nanoparticles or DNR alone.

Fe₃O₄ nanoparticles and DNR increase cell apoptosis through Caspase-8/PARP pathway

K562 and KA cells were both treated with DNR, Fe₃O₄ nanoparticles, or Fe₃O₄ and DNR for 72 hours. Cells were then stained with Acridine Orange/Ethidium Bromide (AO/EB) to detect cell apoptosis. The apoptotic nuclei of K562 and KA were identified by their distinctively fragmented appearance (Fig. 2A). For the control cells without treatment, cell nuclei were normal as shown in Figure 2A (control). The apoptotic rates of K562 cells treated with DNR or Fe₃O₄ were about 22% and 17%, respectively. However, the cell apoptotic rate with Fe₃O₄ nanoparticles and DNR treatments was much higher and reached about 32% (Fig. 2B, K562). Since KA is a drug-resistant cell line, DNR treatment only caused about 13% of cell apoptosis (Fig. 2B, KA). However, the apoptotic rate reached 38% when KA cells were treated with DNR and Fe₃O₄ nanoparticles.

We further confirmed the apoptosis induced by DNR and Fe₃O₄ treatments using DNA fragmentation assay. DNA fragmentations of K562 cells were clearly observed with DNR

treatment (Fig. 3A, K562, lane 2) or with treatment of Fe₃O₄ nanoparticles plus DNR (K562, lane 3). Minimal DNA fragmentation was detected in K562 cells treated with Fe₃O₄ nanoparticles alone (K562, lane 4). Importantly, KA cells treated with Fe₃O₄ nanoparticles and DNR showed a much larger amount of fragmented chromosomal DNA (Fig. 3A, KA, lane 3) than the ones treated with only DNR (KA, lane 2) or Fe₃O₄ nanoparticles (KA, lane 1). Therefore, Fe₃O₄ nanoparticles with DNR significantly enhanced the apoptosis-inducing effect of DNR on leukemia cells, especially on the drug-resistant leukemia KA cells.

To explore the molecular mechanisms underlying the Fe₃O₄/DNR treatment-induced DNA fragmentation, we examined the apoptosis-related protein expression (Fig. 3B). When K562 cells were treated with DNR (Fig. 3B, 2), the cleaved Caspase-8 signals on Western blots were much stronger than that of cells treated with Fe₃O₄ nanoparticles (Fig. 3B, 3). DNR with Fe₃O₄ treatments led to the strongest activation of Caspase-8 (Fig. 3B, 4). Lane 1 in Figure 3B represents the cells without any treatment. Similar results were obtained for cleaved Caspase-7 and cleaved PARP since they are the downstream elements of Caspase-8 pathway. When Poly-(ADP-ribose) polymerase (PARP) is cleaved by caspase activation, it loses its DNA repair function and signals the cells to move into apoptosis. In KA cells, the cleaved Caspase-8 signal was higher in Fe₃O₄ treatment than in DNR treatment due to the drug-resistance nature of the cells (Fig. 3B, 3 and 2, respectively). The combined treatment using DNR and Fe₃O₄ induced the highest level of cleaved Caspase-8 in KA cells. The same trend was obtained for cleaved Caspase-7 and cleaved PARP.

DNR with Fe₃O₄ treatments increase intracellular DNR fluorescence signals

Next, we examined whether Fe₃O₄ nanoparticles increased DNR accumulation in the treated cells. Since DNR emitted a green fluorescence, the number of fluorescent K562 cells was counted by flow cytometry based on the fluorescence intensity after the cells were treated with DNR (Fig. 4A, b) or with Fe₃O₄ nanoparticles and DNR (Fig. 4A, c). The K562 cells without any treatment served as a control (Fig. 4A, a). The quantitative analysis showed that the percentage of fluorescent K562 cells increased dramatically after they went through DNR and Fe₃O₄ treatments compared to that of DNR alone treated cells (Fig. 4A, d, Fe₃O₄+DNR). DNR alone treatment revealed a low number of fluorescent KA cells due to its multidrug resistance (Fig. 4B, b). The fluorescent KA cells increased greatly with DNR and Fe₃O₄ treatments (Fig. 4B, c). Figure 4B(d) is the quantitative analysis of fluorescent KA cells after different treatments. The intracellular DNR fluorescent signals of K562 and KA cells were further assayed with the fluorescent light microscopy. Figure 4C illustrates the typical fluorescent images of K562 (a–c) and KA (d–f) cells with no treatment (a and d), treated with DNR (b and e), or with DNR and Fe₃O₄ (c and f). These results were consistent with the flow cytometry results. These data demonstrated the higher fluorescent intensity in K562 and KA cells treated with DNR and Fe₃O₄ than the cells treated with DNR alone.

Fe₃O₄ nanoparticle and DNR suppressed tumor growth in nude mice

To investigate the effects of Fe₃O₄ nanoparticles and DNR on K562 and K- induced tumorigenesis *in vivo*, nude mice were inoculated with K562 or KA cells and the subsequent tumor growth was recorded after various treatments. K562 mice without any treatment showed the largest tumor volume (3000 mm³, Fig. 5A, group 1). Although Fe₃O₄ alone treatment did not significantly inhibit tumor growth (group 2), DNR alone or Fe₃O₄ with DNR treatments greatly inhibited the tumor growth in K562 mice (group 3 or 4). The group 5 mice were treated with Fe₃O₄ and DNR in the presence of an external magnetic field and the tumor growth was also efficiently suppressed. For the group 6 mice, the tumor growth was moderately suppressed by Fe₃O₄ in the presence of an external magnetic field.

For the KA nude mice, the tumor volume of the control group was increased to almost 5000 mm³ (Fig. 5B, group 1). The tumor size of the mice treated with Fe₃O₄ and DNR (group 4) was significantly reduced compared to that of the control group (group 1) and the groups treated with Fe₃O₄ (group 2) or DNR (group 3) alone. The tumor growth was greatly inhibited in group 5 mice with the same treatment that was used on group 4, but in the presence of an external magnetic field. The group 6 mice were treated with Fe₃O₄ in the presence of an external magnetic field and the tumor growth was moderately suppressed. Treatments with Fe₃O₄ or DNR alone had no significant inhibitory effects on the tumor growth in KA mice (group 2 and 3).

To investigate the distribution of Fe₃O₄ nanoparticles *in vivo*, the tissue uptake of Fe₃O₄ nanoparticles was examined. Figure 4C shows the distribution of Fe levels in various organs. In the case of group 2 mice (treated with DNR only), organ distribution of Fe levels was the same as that of the control group (group 1, no treatment). However, when Fe₃O₄ nanoparticles were injected into nude mice of group 3, 4, and 5, the amount of Fe in all tested organs was higher than the amount in the control group, especially in the liver, intestine, and tumor ($p < 0.05$ compared to the control group). We also measured Fe levels in the blood of all 5 groups of mice. Our data showed that there is no statistically significant increase of Fe in groups 3, 4, and 5 blood samples compared with groups 1 and 2 (data not shown).

Fe₃O₄ nanoparticles and DNR induce cell apoptosis in K562 and KA xenograft tumors

The synergistic effect of Fe₃O₄ nanoparticles with DNR on the apoptosis induction in the xenograft tumors excised from K562 and KA mice was evaluated (Fig. 6). The apoptotic rate in the K562 xenograft tumors without treatment (Fig. 6A, control, group 1) was about 12%. The apoptotic rate in group 2 (treated with Fe₃O₄) did not increase significantly. However, for group 3 (treated with DNR), group 4 (treated with Fe₃O₄ nanoparticle and DNR), and group 5 mice (treated with Fe₃O₄ nanoparticles and DNR in the presence of an external magnetic field), the number of apoptotic cells was considerably higher in comparison to that of the control group 1 (Fig. 6A).

In the xenograft tumors excised from the KA nude mice, the apoptotic rate in the control group 1 was around 12% (Fig. 6B). The number of apoptotic cells increased slightly in group 2 and 3 xenograft tumors (treated with Fe₃O₄ or DNR only), but did not reach a statistically significant level. In group 4 (treated with Fe₃O₄ nanoparticle and DNR) and group 5 xenograft tumors (treated with Fe₃O₄ nanoparticles and DNR in the presence of an external magnetic field), the apoptotic rate increased dramatically, indicating that the treatment was effective. These results demonstrate again that the low concentration of Fe₃O₄ nanoparticles or DNR alone did not efficiently induce cell apoptosis in tumor tissues due to the multidrug resistance of the KA cell line. The result of apoptotic rate correlated well with that of tumor growth inhibition *in vivo*.

Discussion

In this study, we report that Fe₃O₄ nanoparticles increased the ability of DNR to induce apoptosis in both adriamycin-sensitive and adriamycin-resistant K562 cells through Caspase-8/PARP pathway. Furthermore, Fe₃O₄ nanoparticles combined with DNR effectively inhibited the tumor growth induced by the inoculation of K562 cells into nude mice. Our studies clearly showed the significant enhancement of the apoptotic rate by synergistic effect of Fe₃O₄ nanoparticles with DNR on drug resistant leukemia cells.

Certain nanoparticles can cause the formation of “holes” on the surface of cell membranes, which could increase the permeability of the respective cell membranes and thus facilitate

the anti-cancer drugs into cancer cells and enhance the accumulation of relevant molecules in target cells.¹² Indeed, our results showed that, with the increased apoptotic effects of Fe₃O₄ nanoparticles and DNR treatments in K562 and KA cells, DNR was increasingly accumulated in the target cells.

A successful anti-cancer treatment should have the capability to efficiently inhibit cancer cell growth *in vivo*. As shown in our data, Fe₃O₄ nanoparticles or DNR alone was unable to significantly inhibit the tumor growth in KA mice due to the multidrug resistance of this cell line. However, Fe₃O₄ nanoparticles with DNR in the presence of the magnet in KA mice greatly enhanced anti-tumor activity, suggesting the synergetic effect of Fe₃O₄ nanoparticles with DNR. The magnetic field can direct the Fe₃O₄ nanoparticles to the tumor site. We hypothesize that Fe₃O₄ nanoparticles could disrupt the tumor cell membrane so that DNR could be delivered into the tumor cells more efficiently. Many studies also reported that the magnetic field itself could slow down the tumor growth in nude mice, cause DNA damage, and induce cell apoptosis.^{13–14} Future studies are needed to understand the relationships of the magnetic field, nanoparticles, and anti-cancer drugs

Our studies demonstrated that Fe₃O₄ nanoparticles combined with DNR treatments induce apoptosis in both K562/KA cells and tumors. This effect was likely achieved through the activation of Caspase-8 pathway since cleaved Caspase-8, Caspase-7, and PARP were greatly increased after Fe₃O₄ and DNR treatments. It is known that activation of Caspase-8 induces apoptosis through the cleavage of downstream caspases including Caspase-7.¹⁵ Activated Caspase-7 cleaves PARP to elicit apoptosis leading to DNA fragmentation as was demonstrated in our current studies.

We found that Fe concentration in the nude mice injected with Fe₃O₄ nanoparticles was significantly higher in the liver and intestine than in other tissues compared to the control group. According to the results reported by others, the removal of the Fe₃O₄ nanoparticles is accomplished by the liver, which belongs to the reticuloendothelial system (RES).¹⁶ The RES is responsible for removing foreign particles from the circulatory system, and the particles are excreted via intestines. Therefore, our current study suggests that Fe₃O₄ nanoparticles combined with anti-cancer drugs may serve as a potentially viable targeted therapeutic approach for cancer treatments.

Supplementary Material

Refer to Web version on PubMed Central for supplementary material.

Acknowledgments

This work was supported by the National Natural Science Foundation of China (90713023, 20675014, 20535010), National Basic Research Program of China (2010CB732404), National High Technology Research and Development Program of China (2007AA022007), Doctoral Fund of Ministry of Education of China (RFDP 20090092110028), and the Natural Science Foundation of Jiangsu Province (BK2008149) to X. M. W., and the National Institutes of Health grant ES016888 of United States to Y.H.C.

References

1. Lv G, He F, Wang X, Gao F, Zhang G, Wang T, et al. Novel nanocomposite of nano Fe₃O₄ and polylactide nanofibers for application in drug uptake and induction of cell death of leukemia cancer cells. *Langmuir*. 2008; 24:2151–2156. [PubMed: 18193905]
2. Zhang R, Wang X, Wu C, Song M, Li J, Lv G, et al. Synergistic enhancement effect of magnetic nanoparticles on anticancer drug accumulation in cancer cells. *Nanotechnology*. 2006; 17:3622–3626. [PubMed: 19661614]

3. Brigger I, Dubernet C, Couvreur P. Nanoparticles in cancer therapy and diagnosis. *Adv Drug Deliv Rev.* 2002; 54:631–651. [PubMed: 12204596]
4. Kreuter J. Nanoparticulate systems for brain delivery of drugs. *Adv Drug Deliv Rev.* 2001; 47:65–81. [PubMed: 11251246]
5. Gref R, Minamitake Y, Peracchia MT, Trubetskoy V, Torchilin V, Langer R. Biodegradable long-circulating polymeric nanospheres. *Science.* 1994; 263:1600–1603. [PubMed: 8128245]
6. Felix CA. Leukemias related to treatment with DNA topoisomerase II inhibitors. *Med Pediatr Oncol.* 2001; 36:525–535. [PubMed: 11340607]
7. Chau M, Christensen JL, Ajami AM, Capizzi RL. Amonafide, a topoisomerase II inhibitor, is unaffected by P-glycoprotein-mediated efflux. *Leuk Res.* 2008; 32:465–473. [PubMed: 17826829]
8. Wu T, Hua M, Chen J, Wei K, Jung S. Effects of external magnetic field on biodistribution of nanoparticles: A histological study. *Journal of Magnetism and Magnetic Materials.* 2007; 311:372–375.
9. Dresco PA, Zaitsev VS, Gambino RJ, Chu B. Preparation and Properties of Magnetite and Polymer Magnetite Nanoparticles. *Langmuir.* 1999; 15:1945–1951.
10. Ito A, Matsuoka F, Honda H, Kobayashi T. Heat shock protein 70 gene therapy combined with hyperthermia using magnetic nanoparticles. *Cancer Gene Ther.* 2003; 10:918–925. [PubMed: 14712318]
11. Ganta S, Amiji M. Coadministration of Paclitaxel and curcumin in nanoemulsion formulations to overcome multidrug resistance in tumor cells. *Mol Pharm.* 2009; 6:928–939. [PubMed: 19278222]
12. Guo D, Wu C, Li X, Jiang H, Wang X, Chen B. In vitro cellular uptake and cytotoxic effect of functionalized nickel nanoparticles on leukemia cancer cells. *J Nanosci Nanotechnol.* 2008; 8:2301–2307. [PubMed: 18572641]
13. Tofani S, Barone D, Berardelli M, Berno E, Cintorino M, Foglia L, et al. Static and ELF magnetic fields enhance the in vivo anti-tumor efficacy of cis-platin against lewis lung carcinoma, but not of cyclophosphamide against B16 melanotic melanoma. *Pharmacol Res.* 2003; 48:83–90. [PubMed: 12770519]
14. Jajte J, Grzegorzczak J, Zmyslony M, Rajkowska E. Effect of 7 mT static magnetic field and iron ions on rat lymphocytes: apoptosis, necrosis and free radical processes. *Bioelectrochemistry.* 2002; 57:107–111. [PubMed: 12160605]
15. Hu W, Kavanagh JJ. Anticancer therapy targeting the apoptotic pathway. *Lancet Oncol.* 2003; 4:721–729. [PubMed: 14662428]
16. Gaur U, Sahoo SK, De TK, Ghosh PC, Maitra A, Ghosh PK. Biodistribution of fluoresceinated dextran using novel nanoparticles evading reticuloendothelial system. *Int J Pharm.* 2000; 202:1–10. [PubMed: 10915921]

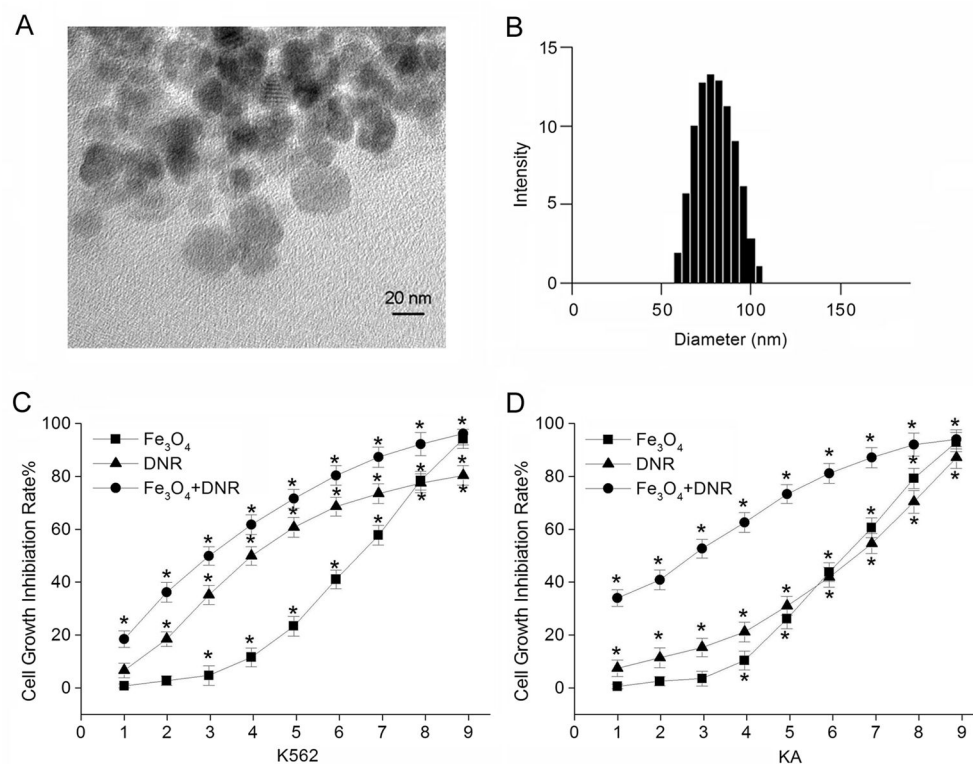


Figure 1.

A. The transmission electron microscopy (TEM) images of Fe₃O₄ nanoparticles. **B.** The size distribution of Fe₃O₄ nanoparticles in the culture medium characterized by Dynamic Light Scattering (DLS). The growth inhibition rate of K562 (**C**) and KA (**D**) cells after various treatments using MTT assays. The K562 cells were treated as follows: 1: 9.93×10^{-7} ; 2: 1.99×10^{-6} ; 3: 3.97×10^{-6} ; 4: 7.94×10^{-6} ; 5: 15.89×10^{-6} ; 6: 31.78×10^{-6} ; 7: 63.55×10^{-6} ; 8: 12.71×10^{-5} ; 9: 25.42×10^{-5} of DNR (mol/L, triangles), or 1: 7.25×10^{-2} ; 2: 1.45×10^{-1} ; 3: 0.29; 4: 0.58; 5: 1.12; 6: 2.24; 7: 4.48; 8: 9.96; 9: 17.92 of Fe₃O₄ nanoparticles (mg/L, squares), or 0.58 mg/L Fe₃O₄ concentration with 1: 9.93×10^{-7} ; 2: 1.99×10^{-6} ; 3: 3.97×10^{-6} ; 4: 7.94×10^{-6} ; 5: 15.89×10^{-6} ; 6: 31.78×10^{-6} ; 7: 63.55×10^{-6} ; 8: 12.71×10^{-5} ; 9: 25.42×10^{-5} of DNR (mol/L, circles), respectively. The KA cells were treated the same way as K562 cells were. *Indicates the significant difference in comparison to no treatment ($p < 0.05$).

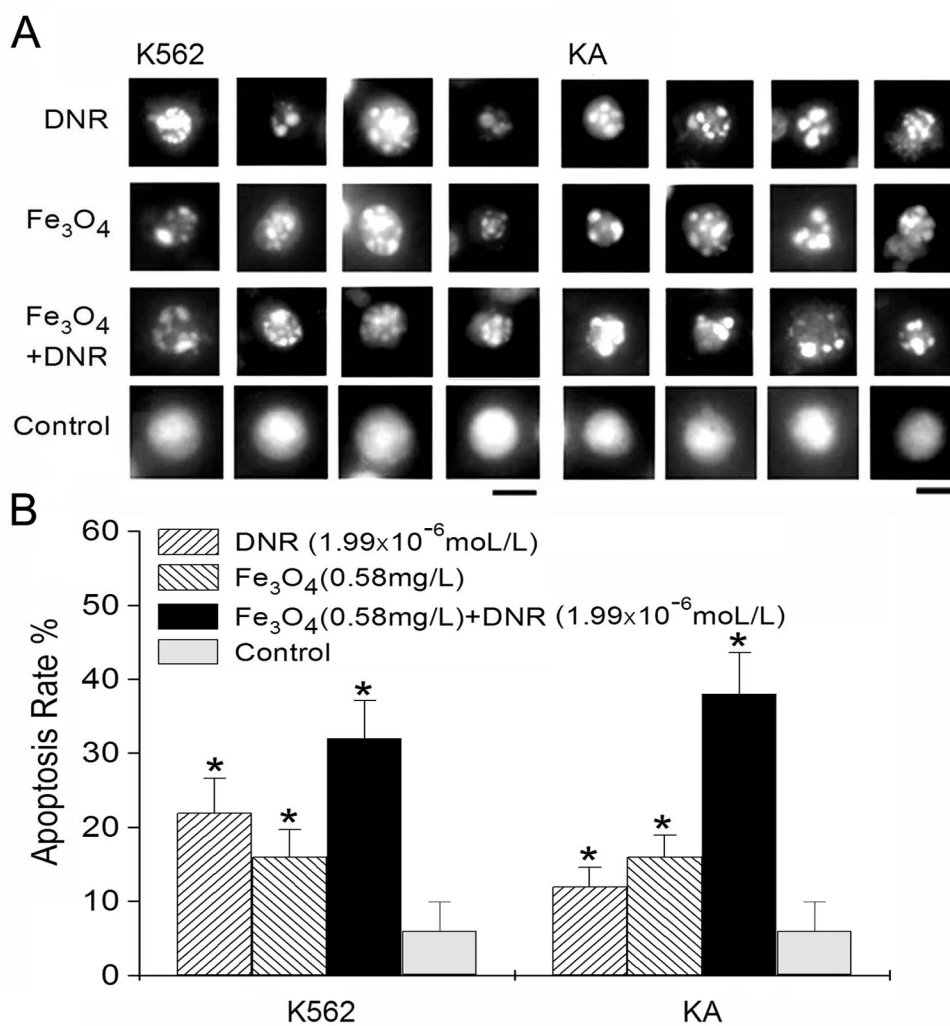


Figure 2.

A. The apoptotic nuclei in K562 and KA cells after 72 h treatments with 1.99×10^{-6} mol/L of DNR (DNR), 0.58 mg/L of Fe_3O_4 nanoparticles (Fe_3O_4), or the same Fe_3O_4 concentration with 1.99×10^{-6} mol/L of DNR (Fe_3O_4 +DNR). Cell nuclei from untreated K562 and KA cells were labeled as controls. Bars: 10 μm . **B.** The apoptotic rate of K562 and KA cells after various treatments as shown in (A). The distinctively fragmented cell nuclei were counted randomly from 15 different fields in each condition. *Indicates the significant difference in comparison to the control ($p < 0.05$).

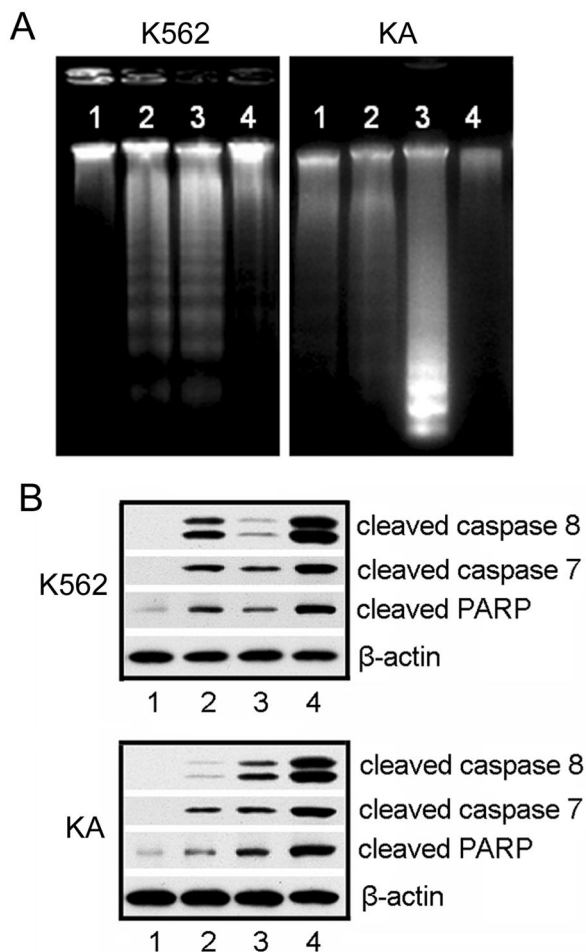


Figure 3.

A. DNA fragmentation in Leukemia cells after different treatments. Genomic DNA was isolated from K562 or KA cells. DNA ladders were visualized under UV light with ethidium bromide staining. K562 cells (a) were treated with: 1, no treatment; 2, 1.99×10^{-6} mol/L DNR; 3, 0.58 mg/L Fe_3O_4 nanoparticles with 1.99×10^{-6} mol/L DNR; 4, 0.58 mg/L Fe_3O_4 nanoparticles. KA cells (b) were treated with: 1, 0.58 mg/L Fe_3O_4 nanoparticles; 2, 1.99×10^{-6} mol/L DNR; 3, 0.58 mg/L Fe_3O_4 nanoparticles with 1.99×10^{-6} mol/L DNR; 4, no treatment. **B.** Western blotting analysis of activated caspases after various treatments. K562 and KA cell lysates were prepared from the cells without treatment (1), treated with 1.99×10^{-6} mol/L DNR (2), 0.58 mg/L Fe_3O_4 nanoparticles (3), or 0.58 mg/L Fe_3O_4 nanoparticles and 1.99×10^{-6} mol/L DNR (4). The following antibodies were used: anti-cleaved Caspase-8, anti-cleaved Caspase-7, and anti-PARP antibody. β -Actin was used as a loading control.

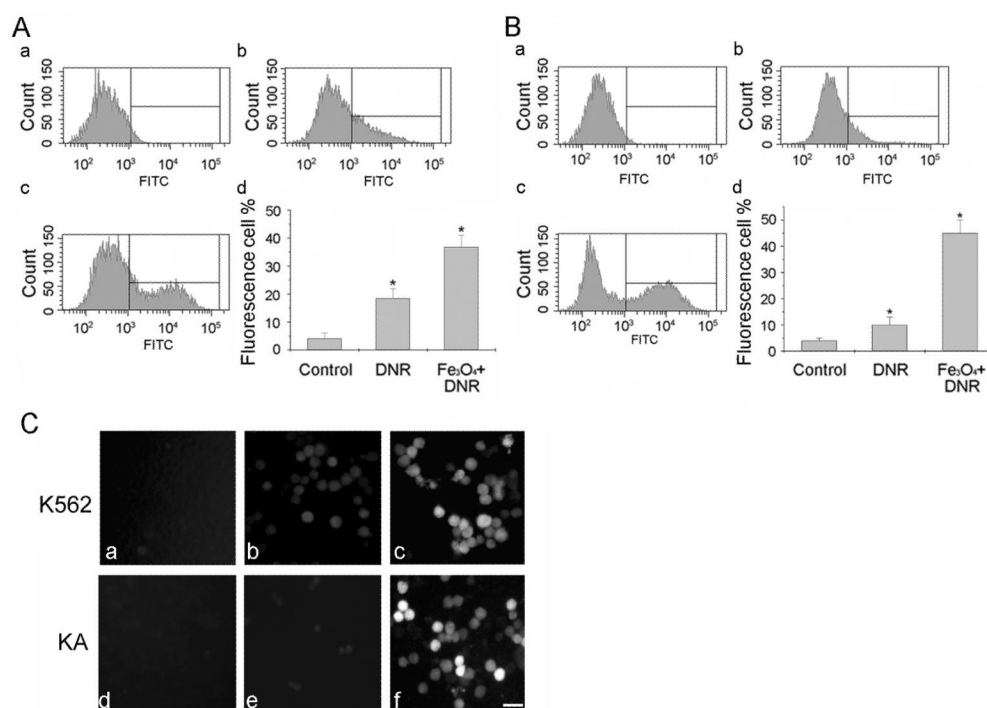
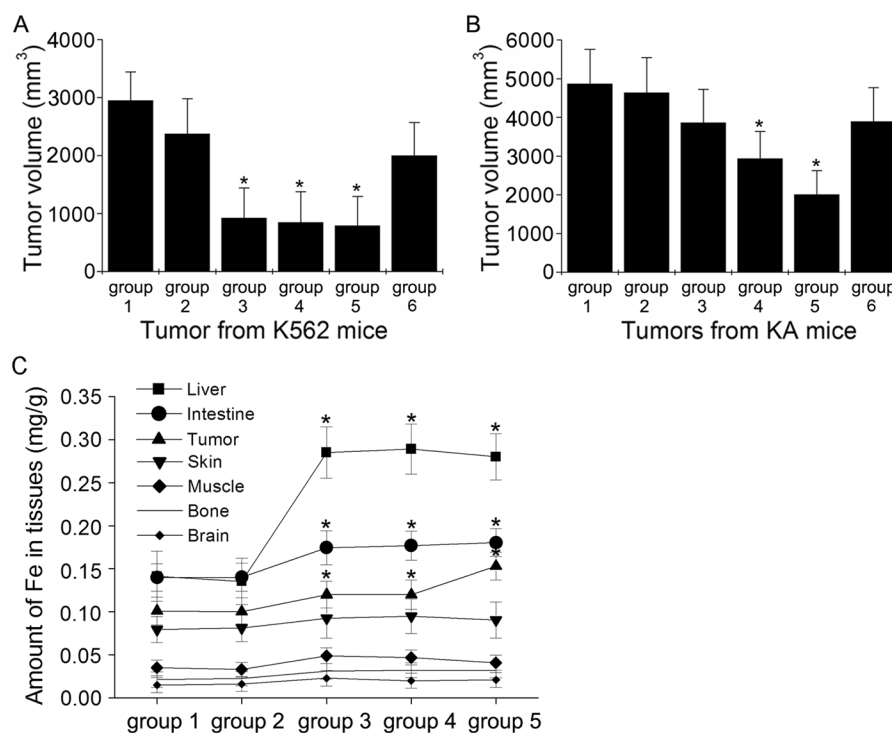


Figure 4. Fluorescence accumulation in K562 (A) and KA cells (B) analyzed by Flow Cytometry with no treatment (control, a), treated with DNR (b), or with Fe₃O₄ nanoparticles and DNR (c). The quantitative analysis of fluorescence cells after various treatments were shown in (d). The results were obtained from three independent experiments. * $P < 0.05$, compared to the control. C. Examples of fluorescence images of K562 (a–c) and KA cells (d–f). Control: a and d; DNR: b and e; Fe₃O₄ and DNR: c and f. Bar: 20 μm .

**Figure 5.**

A. The effect of different treatments on the tumor growth inhibition in nude mice inoculated with K562 cells. Group 1, no treatment; group 2, 0.58 mg/L Fe₃O₄ nanoparticles; group 3, 1.99 × 10⁻⁶ mol/L DNR; group 4, 0.58 mg/L Fe₃O₄ nanoparticles with 1.99 × 10⁻⁶ mol/L DNR; group 5, the same treatment as group 4 plus a magnet fixed securely close to the tumor site; group 6, 0.58 mg/L Fe₃O₄ nanoparticles plus a magnet fixed securely close to the tumor site. **B.** The effect of different treatments on the tumor growth inhibition in nude mice inoculated with KA cells. The 6 groups of mice had the same treatments as shown in (A). Each data point represents the mean ± SD (n = 5). *Indicates significant difference in comparison to the control group 1 (p < 0.05). **C.** Distribution of Fe levels in liver, intestine, tumor, skin, muscle, bone, and brain from different treatment groups. The K562 and KA nude mice were treated the same way as shown in (A) except group 2 with 1.99 × 10⁻⁶ mol/L DNR and group 3 with 0.58 mg/L Fe₃O₄ nanoparticles. *Indicates significant difference in comparison to the control group 1 (p < 0.05).

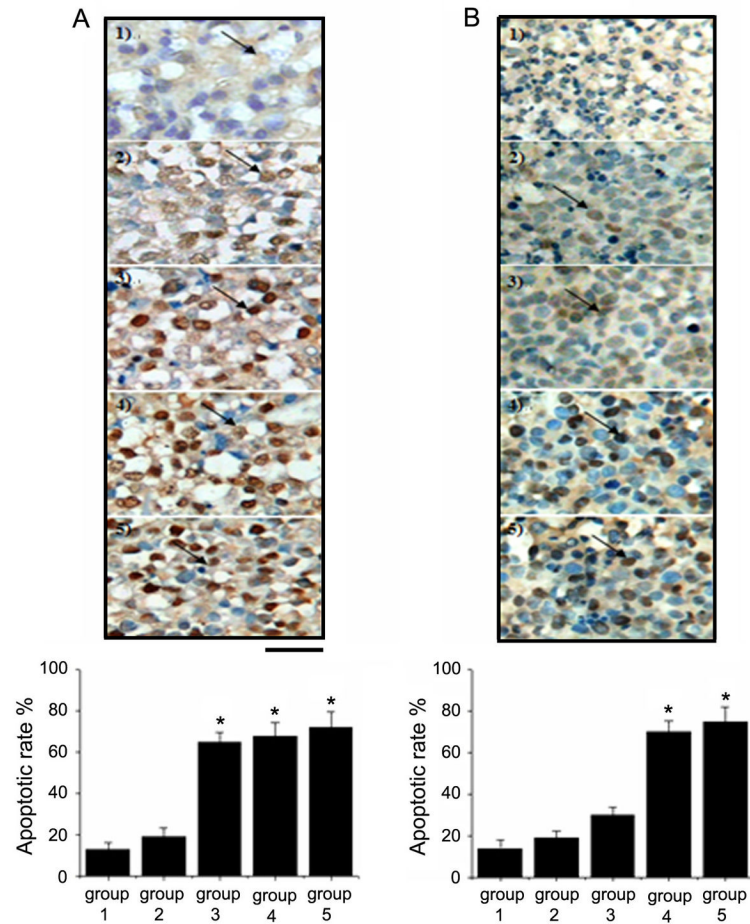


Figure 6.

Immunohistochemical staining of apoptotic cells in K562 and KA xenograft tumors. **A.** TUNEL staining was performed on tissue sections of K562 xenograft tumors treated as follows: group 1, untreated; group 2, 0.58 mg/L Fe₃O₄ nanoparticles; group 3, 1.99 × 10⁻⁶ mol/L DNR; group 4, 0.58 mg/L Fe₃O₄ nanoparticles with 1.99 × 10⁻⁶ mol/L DNR; group 5, with the same treatment as group 4 plus a magnet fixed securely close to the tumor site. **B.** TUNEL staining was performed on tissue sections of KA xenograft tumors. The 5 groups of mice had the same treatments as shown in (A). Arrows: TUNEL positive cells (indicate apoptotic cells). The bar graphs represent the results from three independent experiments. Data are the mean (±SD) number of cells/microscope field from five animals per group. *Indicates significant difference in comparison to the control group ($p < 0.05$).

Table 1IC₅₀ values of DNR, Fe₃O₄, and Fe₃O₄ plus DNR according to the MTT assay

treatment type	IC ₅₀ values	
	K562 cells	KA cells
Fe ₃ O ₄ (mg/L)	3.30±0.25	3.25±0.30
DNR (mol/L)	7.94±0.76×10 ⁻⁶	39.72±2.95×10 ⁻⁶
Fe ₃ O ₄ +DNR (mg/L+mol/L)	0.58 + 3.95×10 ⁻⁶	0.58 + 3.18×10 ⁻⁶

The values are shown as mean±SD, *n* = 5.Note: IC₅₀ values indicate the 50% growth inhibitory concentration values of DNR, Fe₃O₄, and Fe₃O₄ plus DNR.

Table 2Fe₃O₄ and DNR Combination Index (CI) against K562 and KA Cells

combination type	K562 cells		KA cells	
	CI	interaction type	CI	interaction type
Fe ₃ O ₄ +DNR	0.67	synergistic	0.26	synergistic

CI < 1, synergistic; CI = 1, additive; CI > 1, antagonistic.

Table 3

The resistant factors and reversal index of K562 and KA cells to Fe₃O₄ nanoparticles

	IC ₅₀ mol/L		Resistant factors	Reversal Index
	K562	KA		
DNR	7.94±0.76×10 ⁻⁶	39.72±2.95×10 ⁻⁶	5.00	
Fe ₃ O ₄ +DNR	3.95×10 ⁻⁶	3.18×10 ⁻⁶	0.80	6.25

Resistant factor (R_f) = [IC₅₀] KA/[IC₅₀] K562; Reversal index (R_i) = [R_f]/[R_f'], where R_f and R_f' stand for the resistant factor of KA with DNR alone and Fe₃O₄ nanoparticle with DNR, respectively.